

Video2StyleGAN: Disentangling Local and Global Variations in a Video

RAMEEN ABDAL, KAUST, Saudi Arabia
 PEIHAO ZHU, KAUST, Saudi Arabia
 NILOY J. MITRA, UCL and Adobe Research, UK
 PETER WONKA, KAUST, Saudi Arabia

Image editing using a pretrained StyleGAN generator has emerged as a powerful paradigm for facial editing, providing disentangled controls over age, expression, illumination, etc. However, the approach cannot be directly adopted for video manipulations. We hypothesize that the main missing ingredient is the lack of fine-grained and disentangled control over face location, face pose, and local facial expressions. In this work, we demonstrate that such a fine-grained control is indeed achievable using pretrained StyleGAN by working across multiple (latent) spaces (namely, the positional space, the $W+$ space, and the S space) and combining the optimization results across the multiple spaces. Building on this enabling component, we introduce Video2StyleGAN that takes a target image and driving video(s) to reenact the local and global locations and expressions from the driving video in the identity of the target image. We evaluate the effectiveness of our method over multiple challenging scenarios and demonstrate clear improvements over alternative approaches.

CCS Concepts: • **Video Editing** → *Face Reenactment*; • **Neural Rendering** → *Face Editing*; • **Generative Modeling** → *GANs*.

Additional Key Words and Phrases: Generative Adversarial Networks, Video Editing

1 INTRODUCTION

Generative modeling has seen tremendous progress in recent years. Currently, there are multiple powerful frameworks competing in this area, including generative adversarial networks (GANs) [Karras et al. 2020a, 2021a], variational autoencoders (VAEs) [Razavi et al. 2019], diffusion network [Ramesh et al. 2022], and auto-regressive models (ARs) [Esser et al. 2021].

In this paper, we focus on GANs and in particular the StyleGAN architecture. This architecture has started a wave of research exploring semantic image-editing frameworks [Abdal et al. 2021b; Patashnik et al. 2021; Shen et al. 2020]. These frameworks first embed a given photograph into the latent space of StyleGAN and then manipulate the image using latent space operations. Example editing operations in the context of human faces are global parametric image edits to change the pose, age, gender, or lighting, or style transfer operations to convert images to cartoons of a particular style. While these edits are generally successful, it is still an open challenge to obtain fine-grained control over a given face, e.g., face location in the image, head pose, and the facial expression. While such fine-grained control is beneficial but optional for editing single images, they are an essential building block for creating a video from a single image and other video editing applications.

In our work, we set out to address the following research questions: *How can we embed a given video into the StyleGAN latent space to obtain a meaningful and disentangled representation of the video in*

Authors' addresses: Rameen Abdal, KAUST, Saudi Arabia, rameen.abdal@kaust.edu.sa; Peihao Zhu, KAUST, Saudi Arabia, peihao.zhu@kaust.edu.sa; Niloy J. Mitra, UCL and Adobe Research, UK, nimitra@adobe.com; Peter Wonka, KAUST, Saudi Arabia, pwonka@gmail.com.



Fig. 1. **Fine-grained control.** We present Video2StyleGAN, a video editing framework capable of generating videos from a single image. Our framework can take a driving video and transfer its global and local information to a reference image. We build upon the StyleGAN3 architecture to edit the rotation, translation, pose and local expressions independently so that the information can also be derived from multiple videos.

latent space? How can we create a video from a single image, mainly by transferring pose and expression information from other videos?

It is actually somewhat surprising how difficult it is to embed fine grained controls into StyleGAN. However, all straightforward solutions are either over-regularized or under-regularized. Over-regularization leads to the controls being ignored so that the given reference image hardly changes. Under-regularization leads to very unnatural face deformations and identity loss. The main idea of our solution is to make use of different latent spaces to encode different types of information: *positional code* controls the location of the face in the image (i.e. translation and rotation); *W space* controls global edits such as pose and some types of motion; *S space* and generator weights control local and more detailed edits of facial expressions. This hierarchical (code) structure allows the extraction of semantic information from given driving videos and their transfer to a given photograph. See Figure 1.

We compare to a video processing baseline method that does not use multi-resolution latent spaces, as done in recent unpublished arXiv papers [Alaluf et al. 2022; Tzaban et al. 2022].

The contributions of this work are as follows:

- (1) We propose a facial reenactment system that uses the pre-trained StyleGAN3 to transfer the motion and local movements of a talking head that leads to temporally consistent video editing without the requirement of additional training on videos. Our method can transfer these facial movements from a source video onto a single (target) image.
- (2) Our insights into the W and the S space of StyleGAN3 allow us to disentangle both local and global variations in a video. Particularly, we can separately control the eye, nose, and mouth movements. Additionally, we can modify the pose, rotation and translation parameters in a video without compromising the identity of a person.
- (3) Finally, in contrast to previous works that take a single video as an input to modify the facial attributes of a given image, we directly extract the local and global variations from multiple videos to reenact a given image. For example, we are able to modify local features like eye, nose, and mouth variations from one video, and other global features like pose, rotation, and translation derived from another video.

2 RELATED WORK

2.1 State-of-the-art GANs

Recent improvements to the loss functions, architecture and availability of high quality datasets [Karras et al. 2021b] have improved the generation quality and diversity of Generative adversarial Networks (GANs) [Goodfellow et al. 2014; Radford et al. 2015]. Owing to these developments, Karras et. al published a sequence of architectures [Karras et al. 2017, 2020a, 2021a,b, 2020b] leading to state-of-the-art results on high quality datasets like FFHQ [Karras et al. 2021b], AFHQ [Choi et al. 2020] and LSUN objects [Yu et al. 2015]. The latent space learned by these GANs have been explored to perform various tasks such as image editing [Abdal et al. 2019, 2021b; Patashnik et al. 2021; Shen et al. 2020] or unsupervised dense correspondence computation [Peebles et al. 2021]. While recent 3D GANs showed promise in generating high-resolution multi-view-consistent images along with approximate 3D geometry [Chan et al. 2021; Deng et al. 2021; Or-El et al. 2021], their quality still lags behind 2D GANs and code for the best methods is not yet available. In this work, we build upon the state-of-the-art generator StyleGAN3 [Karras et al. 2021a]. StyleGAN3 exhibits nice properties of translation and rotation in-variance with respect to the generated image. These properties attract research into disentangled global and local video editing.

2.2 Image Projection and Editing using GANs

There are two building blocks required for GAN-based image and video editing. First, one needs to project real images into the GAN’s latent space. In the StyleGAN domain, Image2StyleGAN [Abdal et al. 2019] uses the extended $W+$ latent-space to project a real image into the StyleGAN latent space using optimization. Focusing on improving the reconstruction-editing quality trade-off, other methods including I2S [Zhu et al. 2020a] and PIE [Tewari et al. 2020b] propose additional regularizers to make sure the optimization converges to a high density region in the latent space. While other works like IDinvert [Zhu et al. 2020b], pSp [Richardson et al. 2020],

e4e [Tov et al. 2021], and Restyle [Alaluf et al. 2021a] use encoders and identity preserving loss functions to maintain the semantic meaning of the embedding. Two recent works, PTI [Roich et al. 2021] and HyperStyle [Alaluf et al. 2021b] modify the generator weights via an optimization process and Hyper network respectively. Such methods improve the reconstruction quality of the projected images.

Second, latent codes need to be manipulated to achieve a desired edit. For the StyleGAN architecture, InterFaceGAN [Shen et al. 2020], GANSpace [Härkönen et al. 2020], StyleFlow [Abdal et al. 2021b], and StyleRig [Tewari et al. 2020a] propose linear and non-linear edits of the underlying W and $W+$ spaces. StyleSpace [Wu et al. 2020] argues that the S space of StyleGAN leads to better edits. CLIP [Radford et al. 2021] based image editing [Abdal et al. 2021a; Gal et al. 2021; Patashnik et al. 2021] and domain transfer [Chong and Forsyth 2021; Zhu et al. 2022] also study the StyleGAN and CLIP latent spaces to apply StyleGAN based editing on diverse tasks.

2.3 GAN based Video Generation and Editing

GAN based video generation and editing methods [Menapace et al. 2021; Munoz et al. 2020; Tulyakov et al. 2018; Wang et al. 2021] have shown remarkable results on 128×128 , 256×256 and 512×512 spatial resolutions. Owing to the higher resolution and disentangled latent space of the StyleGAN, multiple works in this domain either use the pretrained StyleGAN generator to construct a video generation framework [Alaluf et al. 2022; Fox et al. 2021; Tzaban et al. 2022] or reformulate the problem by training additional modules on top of StyleGAN and using the video data to train the networks [Skorokhodov et al. 2021; Tian et al. 2021; Wang et al. 2022]. Among them is StyleVideoGAN [Fox et al. 2021] which is based on the manipulation in $W+$ space of StyleGAN. Related to the pretrained latent space based method, Third Time’s the Charm [Alaluf et al. 2022] and Stitch it in Time [Tzaban et al. 2022] use the analysis in the W and S spaces of StyleGAN to edit an embedded video. Note that these methods are concurrent to our method and are only available on arXiv at the time of this submission. In addition, these methods solve a different task than ours and are focused on editing an embedded video in different spaces of StyleGAN. Another set of works like StyleGAN-V [Skorokhodov et al. 2021] and LIA [Wang et al. 2022] retrain the modified StyleGAN architecture on videos. Note that our method is a latent space based method on StyleGAN3 trained on images that does not require additional video training. LIA is also trained on different datasets than ours and cannot control the individual components of the generated image by deriving information from different videos. Also note that StyleVideoGAN, Third Time’s the Charm, and Stitch it in Time use $W+$ and/or modified weights of the generator [Roich et al. 2021] to embed videos into the latent space. To compare with such methods, we construct a baseline based on such methods in Sec 4, where $W+$ space is used to encode the global and local components of the video.

3 METHOD

Given a reference image I_{ref} and frames of a driving video D , our goal is to produce a final sequence of video frames $V =: \{V_j\}$ that enacts a talking head with the identity of I_{ref} and pose and expressions, both local and global, from the driving video D . Optionally, a co-driving video $CD := \{CD_j\}$ may be provided as input. We

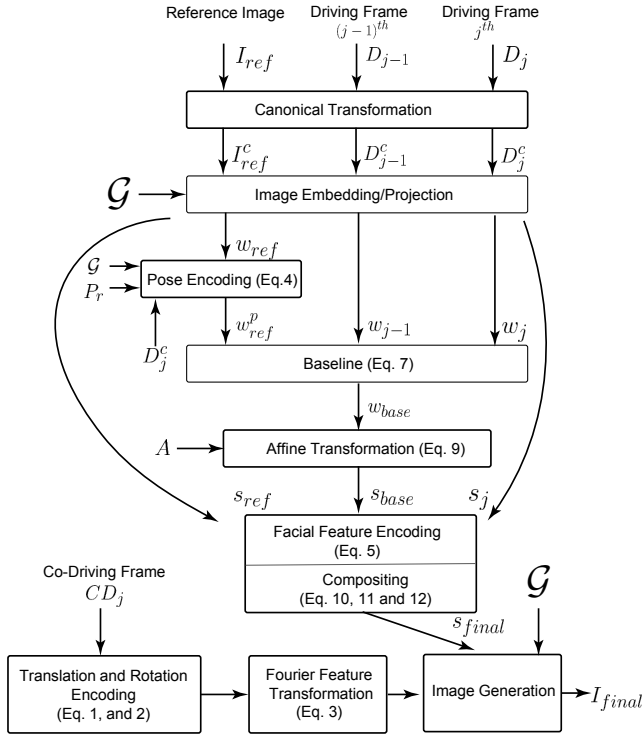


Fig. 2. **Video2StyleGAN pipeline.** Flow diagram of our Video2StyleGAN method. Each box represents a local or global encoding and editing module used by our method. See Section 3 for details.

develop a framework based on these parameters to produce a disentangled representation of a driving video, such that we are able to encode both its global and local properties, and control them separately to produce an output video V .

3.1 Overview

Our framework, see Fig 2, for reenactment of the talking head, using a single (identity) image, is based on the analysis of two spaces associated with StyleGAN3, namely the $W+$ and S spaces. Let $w+ \in W+$ and $s \in S$ be the variables in the respective spaces for any input image. We recall that parameters in the S space are derived from the $w+$ codes using $s := A(w+)$, where A is an affine transformation layer in the StyleGAN3 [Karras et al. 2021a]. Let \mathcal{G} be the pretrained StyleGAN3 generator. In addition to these two latent spaces, we note that the first layer of the StyleGAN3 \mathcal{G} produces interpretable Fourier features, parameterized by translation and rotation parameters. We represent this function as F_f .

Previous research has shown that the $W+$ space [Abdal et al. 2021b] encodes global properties and semantics of an object; while the S space [Wu et al. 2020] is more suited for encoding local variations in a StyleGAN generated image. Based on this observation, we make use of *both* of these spaces in our framework. Specifically, to separately control the local and global variations in our resulting video, we classify such components as local or global editing techniques. Note that some components of the framework includes a

combination of both these spaces to achieve a desirable reenactment (Section 3.5).

In order to encode a given driving video into the latent space of StyleGAN3, we first project the individual frames of the video into the StyleGAN3 latent space. We use the state-of-the-art projection method, ReStyle [Alaluf et al. 2021a] to project the canonical frames of the video and the reference image (i.e., after the FFHQ based transformation) into the $W+$ space ($W+ := \{w+ \in \mathbb{R}^{18 \times 512}\}$) of StyleGAN3. Let the resulting reference image be represented by I_{ref}^c and w_{ref} be the corresponding $w+$ code. In the following subsection, we first introduce the building blocks of our video editing framework, and then combine them to produce Video2StyleGAN, a controllable video generation framework.

3.2 Canonical Transformation

Given a video to define the position of the face within a frame, we exploit the translation and rotation invariance property of the StyleGAN3 architecture to encode the rotation and translation of the talking head. We recall that the Fourier features of StyleGAN3 [Karras et al. 2021a] can be transformed to produce an equivalent effect on the output image. We define a tuple (t_x, t_y, r) , where t_x and t_y are the horizontal and vertical translation parameters, and r is the rotation angle. First, in order to determine the translation and rotation changes from the canonical positions present in FFHQ [Karras et al. 2019], we use a state-of-the-art landmark detector [ageitgey 2018] on each frame of the video to determine the frame-specific (t_x, t_y, r) parameters. For each frame, we compute a vector connecting the average of the positions of the *eye* landmarks and the *mouth* landmarks. We use them to compute the relative angle between the canonical vertical vector and the current face orientation that we use to encode the rotation of the head. Formally, let e_l and e_r be the eye landmarks (left and right, respectively) and m_l be the mouth landmarks predicted by the landmark detector L_d . Then,

$$\vec{e} := 0.5(\mathbb{E}(e_l) + \mathbb{E}(e_r)) \quad \text{and} \quad \vec{v} := \mathbb{E}(m_l) - \vec{e}$$

and

$$r := d_{\cos}(\vec{u}, \vec{v}), \quad (1)$$

where \mathbb{E} denotes average, d_{\cos} is the cosine similarity function, and \vec{u} is the up vector. Similarly, as per the FFHQ transformation, the translation parameters are given by,

$$\vec{t} := \vec{e} - \vec{e}', \quad (2)$$

where \vec{e}' is the midpoint of the canonical FFHQ transformed image, and \vec{t} is a column vector representing t_x and t_y . The transformations



Fig. 3. **Canonical transformation.** Given a driving video (left) with rotation and translation of a driving frame, our framework can transfer this information to a new reference image. Top row: reference images. Bottom row: transformed images.

can then be performed on the Fourier features F_f to produce the desired rotation and translation effects on a given image, as,

$$F'_f(t_x, t_y, r) := F_f(\tau(t_x, t_y, r)) \quad (3)$$

where τ represents the transformation. See Fig. 3 for visual results.

These transformations [Alaluf et al. 2022], however, are not smooth across the frames. Hence, in order to smoothen out the anomalies, we apply a convolution operation to this sequence of parameters across the time domain. Empirically, we found a mean filter with a kernel size of 3 or higher to produce a smooth consistent video after the transformations are applied. Note that these parameters can also be derived from another co-driving video CD , other than the driving video D , and applied to a given image without affecting the identity. For example, we could apply the steps mentioned in the following section from a first driving video and apply the rotation and translation effects from a second co-driving video.



Fig. 4. **Editing global pose.** Given a reference image and a driving frame, we match the pose and local information. Each row shows an identity (reference image) and edits corresponding to the top row (driving frame).

3.3 Global Pose Encoding

Next, we encode the pose of the face in the driving video. We consider this also as a global variation of the video editing framework. Pose changes in StyleGAN are largely associated with adding new details – stretching, squeezing, and transforming the eyes and mouth views to a target position. For this reason, we use the $W+$ space of the StyleGAN3 to encode such global information. Given the hierarchical structure of the StyleGAN3 architecture and semantic understanding of the latent space [Abdal et al. 2021b], we restrict encoding the pose information in the first 8 (out of 16) layers of the StyleGAN3 latent space. First, we observe that when we render the given image by transferring the first two layers of the $w+$ code of a driving frame ($w+ \in W+$), it stretches the face area and the eye, however mouth and nose positions remain unchanged making the output face unrealistic. While transferring the first eight layers makes a plausible pose change at the cost of identity loss (see supplementary video).

To circumvent this, we setup an optimization to match the pose information. Specifically, we setup an objective to optimize for pose (i.e., yaw, pitch, and roll) of a given image to match the pose of the driving video. We propose two loss functions to ensure the pose matching and identity preservation, respectively. To ensure

pose preservation, we use a pose regression model [cunjian 2019] which, given a valid frame of video, outputs yaw, pitch, and roll. To ensure identity preservation, we apply an additional loss to ensure the features of the face and the identity are preserved. The latter loss ensures that the optimized latents from the first 8 layers remain as close to the original latents of a given image as possible. Note that for editing real faces from photographs, we use a PTI based method [Roich et al. 2021] to project the images. In this case, there are multiple ways to optimize the code and we observed that optimizing the code with the original generator for pose and then using the PTI trained generator to fill in the details works the best. The optimization is given by:

$$w_{ref}^p := \arg \min_{w_{ref}^{1:8}} \underbrace{L_{mse}(P_r(G(w_{ref})), P_r(D_j))}_{\text{pose preservation}} + \underbrace{L_1(w_{ref}^{1:8}, w_{ref}^{p1:8})}_{\text{identity preservation}}, \quad (4)$$

where $w_{ref}^{1:8}$ represents the $w+$ code of the reference image for the first eight layers of StyleGAN3, L_{mse} represents the MSE loss, and P_r is the output of the pose regression model [cunjian 2019].

In Fig. 4, we show the results of the pose matching from a random frame in the driving video. The figure shows different results of pose changes made to the reference images under a given pose scenario in the driving video.

3.4 Local Facial Feature Encoding

After encoding the global information in a video, i.e., rotation, translation, and pose of the talking head, the next step is to focus on local information. We identified three semantic parts, namely *eyes*, *mouth*, and *nose*, as being responsible for local changes in a talking head driving video. Note that often expression changes result in coupled variations across these semantic regions. In order to capture the local variances of these semantic parts of the face, we resort to our analysis in the S space of the StyleGAN3 architecture. In order to appreciate the disentangled nature of the S space in StyleGAN3, we encourage the reader to refer to the video of a UI application in the supplementary material showing the local properties of S space and the corresponding feature maps, which can be edited. Just for demonstration, we manually change the S parameter of a given channel of a given layer of StyleGAN3 to observe the desired effect



Fig. 5. **Extracting local facial features.** A given image and some normalized feature maps extracted by the Local Facial Feature Encoding of our framework (see Eq 6). The top row shows maps focusing on the eyes, the middle row shows maps focusing on the nose, and the bottom row shows images focusing on the mouth areas. We restrict latent space optimization to discovered channels responsible for the corresponding edits.

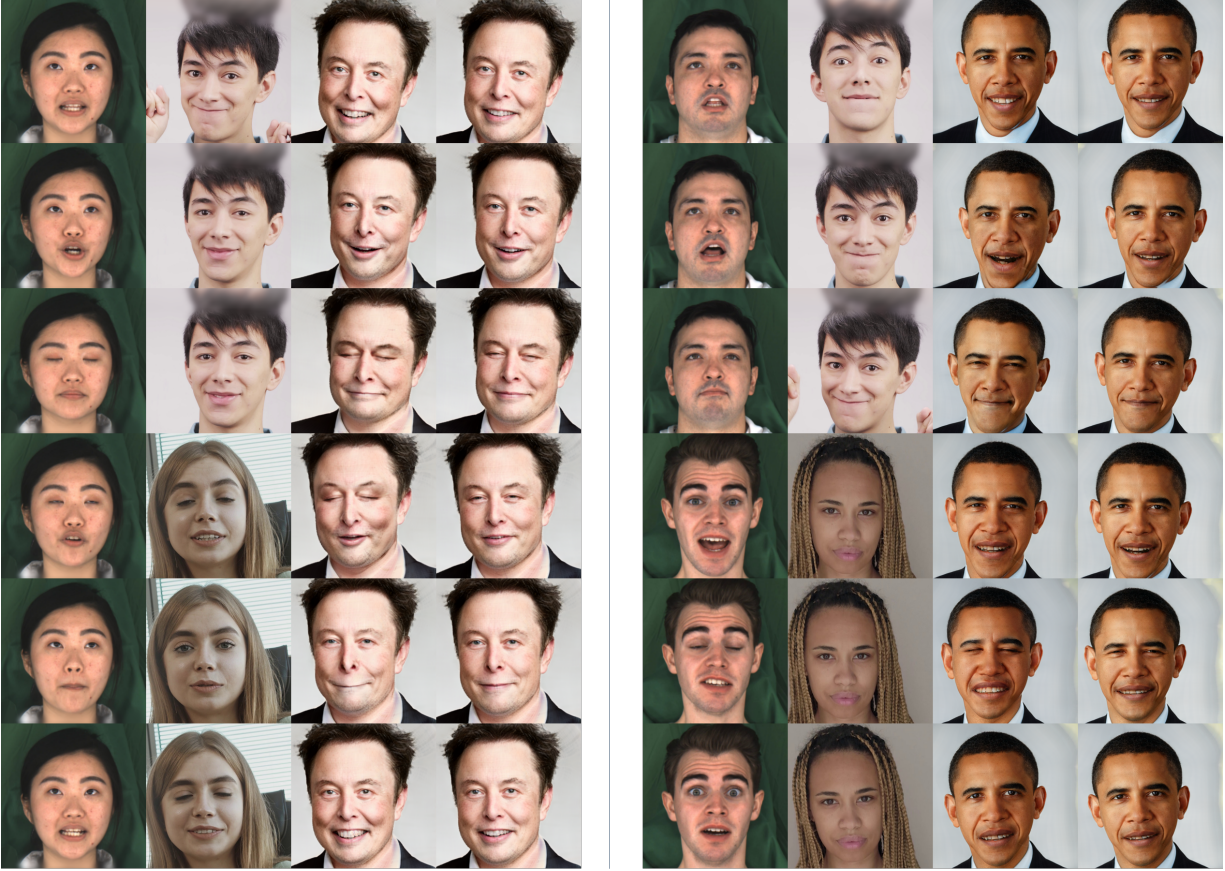


Fig. 6. **Comparison with the baseline.** In each sub-figure, the first column shows the driving frames, the second column shows the co-driving frames, the third column shows the results of the baseline method, and the last column shows our results. Please see the supplementary video.

on the final image. We now use this observation for an automatic procedure for manipulating parameters in the S space.

In order to automatically identify the feature maps and the corresponding $s \in S$ parameters responsible for affecting the motion of the semantic regions, we match the activations in these layers with semantic segmentation regions obtained using a segmentation network. We use a semantic part segmentation network, BiSeNet [Yu et al. 2018], trained on the CELEBA-HQ [Karras et al. 2017] dataset, to determine such layers. First, given a set of images and their feature maps extracted from the StyleGAN3, we first compute the segmentation map of the image using BiSeNet. Second, we compute the normalized maps using min – max normalization per feature channel of the feature maps. Third, to match the spatial size of these masks, we upsample these masks to match the spatial size of the target mask using bilinear interpolation. In order to convert these normalized features into hard masks, we threshold these maps to be binary. Finally, we compute the IOU scores of the three semantic components derived from the set of images by comparing with these binary masks.

Let $SegNet$ be the semantic part segmentation network (e.g., BiSeNet), M_{fg} be the semantic component in consideration, M_{bg} be other semantic components including background given by $SegNet(I_{ref}^c)$.

Let C_l be the feature map at layer l of StyleGAN3 after applying the min – max normalization, upsampling and binarization to the map, to produce,

$$\begin{aligned} IOU^+ &:= IOU(M_{fg}, SegNet(C_l)) \quad \text{and} \\ IOU^- &:= IOU(M_{bg}, SegNet(C_l)). \end{aligned} \quad (5)$$

Based on both the positive IOU^+ (eye, nose, and mouth) and negative IOU^- (background and components excluding the given semantic part) IOU -s, we select a subset of these maps ($\mathcal{X}_m := \{x \in \mathbb{R}^{1024^2}\}$) and the corresponding s parameters ($\mathcal{X}_s := \{x \in \mathbb{R}\}$) based on thresholding to be our local model for the manipulation of the semantic parts. Formally,

$$C_l \in \mathcal{X}_m, \text{ if } IOU^+ \geq t_{fg} \text{ and } IOU^- \geq t_{bg} \quad (6)$$

where t_{fg} and t_{bg} are the thresholds. Note that $\mathcal{X}_s \subset S$. In Fig. 5, we show some examples of the extracted feature maps in \mathcal{X}_m focusing on only a specific semantic part of the face.

3.5 Baseline Video Editing

In our experiments, we found that it is sufficient to simply encode the above global and local components to perform realistic video editing using the StyleGAN3 generator. We observe that even though the

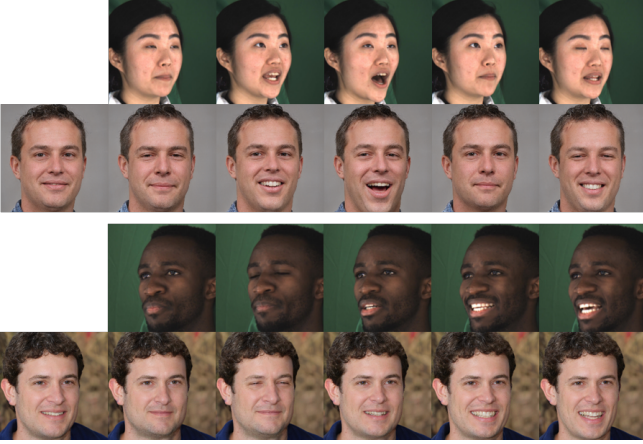


Fig. 7. **Fine-grained local control.** Local information transfer without the global changes like pose. In each sub-figure, top row represents driving frames and the bottom row shows a reference image and local edits.

$w+$ code of the projected driving video can encode non-semantic components, which cannot be directly used for the video editing, it carries other important information that is lost when shifting to the S space analysis described above. Specifically, in Fig. 6, we simply compute the difference vectors in the consecutive frames of the driving video, and apply these transformations to the given latent representing a given image. Formally,

$$w_{base} = w_{ref}^p + (w_{j-1} - w_j) \quad (7)$$

where w_{j-1} is the $w+$ code corresponding to D_{j-1} and w_j is the $w+$ code corresponding to D_j of the driving video.

Notice the artifacts and loss in the identity of the person using such a naive technique for the video editing (see supplementary video). We regard this as a baseline for our method. Nevertheless, we observe that the $w+$ code, despite having some undesirable effects, captures some additional semantics essential for making the motion of the face consistent with the driving video. For example, we observe non-local effects such as stretching and squeezing of the cheek during the movements in the mouth, eye regions, and in the chin. Such coupling between the (semantic) parts cannot be captured by only a local analysis.

3.6 Video2StyleGAN Method

We now combine all these components to present our Video2StyleGAN (see Figure 2). Note that in our framework, components can be separately controlled and driven by multiple videos (see Section 4).

First, we canonicalize the input video(s) by computing the rotation and translation parameters of the driving or a co-driving video using the Translation and Rotation Encoding (Section 3.2), and use the extracted transforms on the given image. Alternatively, we can omit these changes to stay faithful to the original parameters in a given image.

Then, we perform pose changes via the driving or co-driving video using Pose Encoding (Section 3.3). Again, we can omit such changes, i.e., use the pose of the given image without matching it to a driving frame.

Finally, we combine the components of the $W+$ space (Section 3.4) and S space analysis (Section 3.5) to achieve fine-grained control over the video generation. In particular, the degree of local changes can be modified by the $s_{ref}^p \in \mathcal{X}_s$ and combined with the $W+$ space analysis based method. In practice, we identify the $W+$ code layers 3 – 7 to produce best results when combined with the S space. Let $\mathcal{X}_{orig} := \{x \in \mathbb{R}^{512}\}$ be the original $w+$ encoding of the given image using layers 3 – 7. Similarly, we denote another set of $w+$ codes obtained from Eq 7 as $\mathcal{X}_w := \{x \in \mathbb{R}^{512}\}$. Let A_l be the affine function of layer l of the StyleGAN3 generator. Then, we compute the original s parameters as:

$$\mathcal{X}_{origs} := \bigcup_{i=3}^7 A_l(w_l), \quad (8)$$

where $w_l \in \mathcal{X}_{orig}$. Similarly, we compute the s parameter contribution of edited frames as :

$$\mathcal{X}_{ws} := \bigcup_{i=3}^7 A_l(w'_l), \quad (9)$$

where $w'_l \in \mathcal{X}_w$.

We encode the local changes by adding the computed s parameters of the given image (\mathcal{X}_s , see Section 3.3) and a given frame of the driving video (\mathcal{X}_{sd}). Formally, let $s_{ref}^p \in \mathcal{X}_s$ and let $s_j^p \in \mathcal{X}_{sd}$ be the s parameters in the given sets, then the operation is given by:

$$s_{local} = \alpha s_{ref}^p + \beta s_j^p. \quad (10)$$

Combining the two, we define the manipulations:

$$s_{final} = s_{local} + \gamma s_{base}^p, \quad (11)$$

where $s_{base}^p \in \mathcal{X}_{ws}$, such that it matches the s parameter position computed in set \mathcal{X}_s . For other s parameters:

$$s_{final} = \zeta s_{ref}^q + (1 - \zeta) s_{base}^q \quad (12)$$

where $s_{ref}^q \in \mathcal{X}_{origs}$ and $s_{base}^q \in \mathcal{X}_{ws}$. Note that $\alpha, \beta, \gamma, \zeta$ can be controlled separately to produce a desirable animation.

4 RESULTS

4.1 Training and Implementation details

We use an Nvidia A100 GPU for the experiments. We use the R-Config model of the StyleGAN3 for the inference. Starting from a pose in the reference frame, Pose Encoding takes under 1 minute to converge. We set the yaw, pitch, and roll loss weights to 2 and the identity preservation loss weight to 0.04. As a default setting, we set $\alpha = -1$, $\beta = 1$, $\gamma = 1$ and $\zeta = 0.5$.

4.2 Baseline

As a baseline method, we resort to Eq. 7 as method to make consecutive edits to the $w+$ code of the embedded video. Note that this method is widely used by Gan-based image editing methods like InterfaceGAN [Shen et al. 2020] and GANSpace [Härkönen et al. 2020]. More specifically, current video editing works on arXiv [Alaluf et al. 2022; Tzaban et al. 2022] use the videos embedded in the $W+$ space and/or weights of the generator [Roich et al. 2021] to do further editing. We apply the same approach to modify a single image and

generate a video using the driving and the co-driving frames. In Fig 6, third column in each sub-figure shows the result of the baseline method on two different identities.

4.3 Metrics

We use three metrics to evaluate the keypoints, identity preservation, and the quality of the frames in the resulting video. We also check the consistency of these metrics on the resulting videos (Sec 4.5) by encoding a reverse driving video. These metrics are:

- (1) **Keypoint Distance (ΔK):** In order to measure the target edits made to the resulting video we use the Mean Squared Error between the keypoints of the driving video and the resulting video. The keypoint detector [cunjian 2019] predicts 68 keypoints given an image. We average the errors for these 68 keypoints.
- (2) **Identity distance ID :** We use a state-of-the-art Face recognition model [ageitgey 2018] to compute the facial embeddings of the given reference image and the frames of the resulting video. We compute $L2$ norm of these embeddings and take an average across all frames of the video.
- (3) **Fréchet Inception Distance (FID):** FID is used to measure the distance between a given distribution of images to a generated one. In the context of video editing, we use FID as a metric that computes the quality and consistency of the edits made to the given reference frames. This measures how much does the distribution of the resulting frames change under different edits (e.g., by reversing the driving video).

4.4 Qualitative Comparison

In order to visualize the quality of the resulting video, in Figure 1, we show the results of our Video2StyleGAN method on different identities. Note that here we first match the pose of the given identity image to a driving frame and then we apply the local and global edits including the rotation and translation derived from a co-driving video. Notice the quality of the identity preservation across different editing scenarios. To compare our method with the baseline, in Fig 6, we show the results of the editing and transformations. For embedding a real image, we use the Restyle method to produce an embedding and further optimize the generator using PTI [Roich et al. 2021] by initializing with the computed Restyle embedding. Notice that the baseline approach tends to change different features like skin color and produces noticeable artifacts. In comparison, our method is able to preserve the identity of the person and successfully transfer the edits from the driving and the co-driving video. In order to show that our method works when the pose of the reference image does not match the driving frame, in Fig 7, we show the transfer of the local information from the driving frames to a reference image. Notice the quality of edits and identity preservation in these case. Please refer to the supplementary video.

4.5 Quantitative Comparison

In order to compute the metrics on frames of the video produced by our Video2StyleGAN method and compare with the baseline, we use 5 identities to produce a video of 160 frames using the video collected from the MEAD [Wang et al. 2020] dataset. To test the

Table 1. **Quantitative evaluation.** Table showing the evaluation of the Keypoint Distance (ΔK), Identity Distance ID , and FID scores on the baseline method and ours. Lower is better for all the metrics. Here superscript f represents a metric evaluated on a forward driving video and r represents the scores on the reverse driving video. Subscripts x and y represent the evaluation of the two 2D coordinates of the keypoints. See text for details.

Method	ΔK_x^f	ΔK_y^f	ΔK_x^r	ΔK_y^r	ID^f	ID^r	FID
Baseline	0.19	0.40	0.26	0.28	0.46	0.51	17.34
Ours	0.17	0.36	0.20	0.29	0.24	0.23	6.15

consistency of the methods, in addition to computing the edits in the forward direction, we reverse the driving video and compute the edits using this reverse driving video. A consistent method should produce similar edits starting from a reference image, such that the identity, keypoints and the quality of the edits are preserved. In Table 1, we compute the three metrics ΔK , ID and FID using both the driving as well as the reverse driving video. In case of Keypoint Distance (ΔD) (computed for both x and y positions of the keypoints) notice that our method beats the baseline method in both scenarios showing that our method is both better at matching the keypoints as well as consistent across the driving video direction. Similarly, Identity Distance (ID) in our case is much better than the baseline and is consistent across the driving video direction. Finally, in order to compute the quality and consistency of the edits, we measure the FID score between the frames produced by a driving video and its reverse version. The table shows that our results are better in this case as well. This indicates that our method is able to produce consistent quality of images across different identities.

5 CONCLUSIONS

We introduced a framework for fine-grained control for manipulating a single image using the StyleGAN3 generator. In particular, the framework is useful to edit a single image given a driving video. This problem is very challenging, because existing methods either strongly overfit or underfit the driving video. Our experiments yield qualitative results in the accompanying video and quantitative results using three different metrics to demonstrate a clear improvement over the current state of the art, including recent arXiv papers. Our work also has some limitations. Our method is image-based, and we do not reconstruct a complete 3D model. This means we trade 3D and viewpoint consistency for a higher visual quality of details. Further, our algorithm currently only considers face models. Being able to handle complete human bodies would require further extensions. In future work, we would like to explore video editing using other generative models, such as auto-regressive transformer and diffusion. We also propose text driven video editing as a possible direction for future work.

ACKNOWLEDGMENTS

We would like to thank Visual Computing Center (VCC), KAUST for the support, gifts from Adobe Research, and the UCL AI Centre.

REFERENCES

Rameen Abdal, Yipeng Qin, and Peter Wonka. 2019. Image2stylegan: How to embed images into the stylegan latent space?. In *Proceedings of the IEEE/CVF International*

- Conference on Computer Vision*. IEEE, Seoul, Korea, 4432–4441.
- Rameen Abdal, Peihao Zhu, John Femiani, Niloy J. Mitra, and Peter Wonka. 2021a. CLIP2StyleGAN: Unsupervised Extraction of StyleGAN Edit Directions. *CoRR* abs/2112.05219 (2021). arXiv:2112.05219 <https://arxiv.org/abs/2112.05219>
- Rameen Abdal, Peihao Zhu, Niloy J. Mitra, and Peter Wonka. 2021b. StyleFlow: Attribute-Conditioned Exploration of StyleGAN-Generated Images Using Conditional Continuous Normalizing Flows. *ACM Trans. Graph.* 40, 3, Article 21 (may 2021), 21 pages. <https://doi.org/10.1145/3447648>
- ageitgey. 2018. face-recognition. https://github.com/ageitgey/face_recognition
- Yuval Alaluf, Or Patashnik, and Daniel Cohen-Or. 2021a. ReStyle: A Residual-Based StyleGAN Encoder via Iterative Refinement. In *Proceedings of the IEEE/CVF International Conference on Computer Vision (ICCV)*.
- Yuval Alaluf, Or Patashnik, Zongze Wu, Asif Zamir, Eli Shechtman, Dani Lischinski, and Daniel Cohen-Or. 2022. Third Time's the Charm? Image and Video Editing with StyleGAN3. *CoRR* abs/2201.13433 (2022). arXiv:2201.13433 <https://arxiv.org/abs/2201.13433>
- Yuval Alaluf, Omer Tov, Ron Mokady, Rinon Gal, and Amit H. Bermano. 2021b. HyperStyle: StyleGAN Inversion with HyperNetworks for Real Image Editing. *CoRR* abs/2111.15666 (2021). arXiv:2111.15666 <https://arxiv.org/abs/2111.15666>
- Eric R. Chan, Connor Z. Lin, Matthew A. Chan, Koki Nagano, Boxiao Pan, Shalini De Mello, Orazio Gallo, Leonidas Guibas, Jonathan Tremblay, Sameh Khamis, Tero Karras, and Gordon Wetzstein. 2021. Efficient Geometry-aware 3D Generative Adversarial Networks. arXiv:2112.07945 [cs.CV]
- Yunjey Choi, Youngjung Uh, Jaejun Yoo, and Jung-Woo Ha. 2020. StarGAN v2: Diverse Image Synthesis for Multiple Domains. In *Proceedings of the IEEE Conference on Computer Vision and Pattern Recognition*.
- Min Jin Chong and David A. Forsyth. 2021. JoJoGAN: One Shot Face Stylization. *CoRR* abs/2112.11641 (2021). arXiv:2112.11641 <https://arxiv.org/abs/2112.11641>
- cunjian. 2019. pytorch-face-landmark. https://github.com/cunjian/pytorch_face_landmark
- Yu Deng, Jiaolong Yang, Jianfeng Xiang, and Xin Tong. 2021. GRAM: Generative Radiance Manifolds for 3D-Aware Image Generation. arXiv:2112.08867 [cs.CV]
- Patrick Esser, Robin Rombach, and Björn Ommer. 2021. Taming Transformers for High-Resolution Image Synthesis. In *CVPR*.
- Gereon Fox, Ayush Tewari, Mohamed Elgharib, and Christian Theobalt. 2021. Style-VideoGAN: A Temporal Generative Model using a Pretrained StyleGAN. <https://vc.ai.mpi-inf.mpg.de/projects/stylevideogan>
- Rinon Gal, Or Patashnik, Haggai Maron, Gal Chechik, and Daniel Cohen-Or. 2021. Stylegan-nada: Clip-guided domain adaptation of image generators. *arXiv preprint arXiv:2108.00946* (2021).
- Ian J. Goodfellow, Jean Pouget-Abadie, Mehdi Mirza, Bing Xu, David Warde-Farley, Sherjil Ozair, Aaron Courville, and Yoshua Bengio. 2014. Generative Adversarial Networks. arXiv:1406.2661 [stat.ML]
- Erik Härkönen, Aaron Hertzmann, Jaakko Lehtinen, and Sylvain Paris. 2020. Ganspace: Discovering interpretable gan controls. *arXiv preprint arXiv:2004.02546* (2020).
- Tero Karras, Timo Aila, Samuli Laine, and Jaakko Lehtinen. 2017. Progressive Growing of GANs for Improved Quality, Stability, and Variation. arXiv:1710.10196 [cs.NE]
- Tero Karras, Miika Aittala, Janne Hellsten, Samuli Laine, Jaakko Lehtinen, and Timo Aila. 2020a. Training Generative Adversarial Networks with Limited Data. In *Proc. NeurIPS*.
- Tero Karras, Miika Aittala, Samuli Laine, Erik Härkönen, Janne Hellsten, Jaakko Lehtinen, and Timo Aila. 2021a. Alias-Free Generative Adversarial Networks. arXiv:2106.12423 [cs.CV]
- Tero Karras, Samuli Laine, and Timo Aila. 2019. A style-based generator architecture for generative adversarial networks. In *Proceedings of the IEEE/CVF Conference on Computer Vision and Pattern Recognition*. 4401–4410.
- Tero Karras, Samuli Laine, and Timo Aila. 2021b. A Style-Based Generator Architecture for Generative Adversarial Networks. *IEEE transactions on pattern analysis and machine intelligence* 43, 12 (Dec. 2021), 4217–4228. <https://doi.org/10.1109/TPAMI.2020.2970919>
- Tero Karras, Samuli Laine, Miika Aittala, Janne Hellsten, Jaakko Lehtinen, and Timo Aila. 2020b. Analyzing and Improving the Image Quality of StyleGAN. In *Proc. CVPR*.
- Willi Menapace, Stéphane Lathuilière, Sergey Tulyakov, Aliaksandr Siarohin, and Elisa Ricci. 2021. Playable Video Generation. *CoRR* abs/2101.12195 (2021). arXiv:2101.12195 <https://arxiv.org/abs/2101.12195>
- Andres Munoz, Mohammadreza Zolfaghari, Max Argus, and Thomas Brox. 2020. Temporal Shift GAN for Large Scale Video Generation. <https://doi.org/10.48550/ARXIV.2004.01823>
- Roy Or-El, Xuan Luo, Mengyi Shan, Eli Shechtman, Jeong Joon Park, and Ira Kemelmacher-Shlizerman. 2021. StyleSDF: High-Resolution 3D-Consistent Image and Geometry Generation. arXiv:2112.11427 [cs.CV]
- Or Patashnik, Zongze Wu, Eli Shechtman, Daniel Cohen-Or, and Dani Lischinski. 2021. StyleCLIP: Text-Driven Manipulation of StyleGAN Imagery. arXiv:2103.17249 [cs.CV]
- William Peebles, Jun-Yan Zhu, Richard Zhang, Antonio Torralba, Alexei Efros, and Eli Shechtman. 2021. GAN-Supervised Dense Visual Alignment. arXiv:2112.05143 [cs.CV]
- Alec Radford, Jong Wook Kim, Chris Hallacy, Aditya Ramesh, Gabriel Goh, Sandhini Agarwal, Girish Sastry, Amanda Askell, Pamela Mishkin, Jack Clark, Gretchen Krueger, and Ilya Sutskever. 2021. Learning Transferable Visual Models From Natural Language Supervision. *CoRR* abs/2103.00020 (2021). arXiv:2103.00020 <https://arxiv.org/abs/2103.00020>
- Alec Radford, Luke Metz, and Soumith Chintala. 2015. Unsupervised Representation Learning with Deep Convolutional Generative Adversarial Networks. arXiv:1511.06434 [cs.LG]
- Aditya Ramesh, Prafulla Dhariwal, Alex Nichol, Casey Chu, and Mark Chen. 2022. Hierarchical Text-Conditional Image Generation with CLIP Latents.
- Ali Razavi, Aaron van den Oord, and Oriol Vinyals. 2019. Generating Diverse High-Fidelity Images with VQ-VAE-2. In *Advances in Neural Information Processing Systems*, H. Wallach, H. Larochelle, A. Beygelzimer, F. d'Alché-Buc, E. Fox, and R. Garnett (Eds.).
- Elad Richardson, Yuval Alaluf, Or Patashnik, Yotam Nitzan, Yaniv Azar, Stav Shapiro, and Daniel Cohen-Or. 2020. Encoding in Style: a StyleGAN Encoder for Image-to-Image Translation. *arXiv preprint arXiv:2008.00951* (2020).
- Daniel Roich, Ron Mokady, Amit H Bermano, and Daniel Cohen-Or. 2021. Pivotal Tuning for Latent-based Editing of Real Images. *arXiv preprint arXiv:2106.05744* (2021).
- Yujun Shen, Ceyuan Yang, Xiaoou Tang, and Bolei Zhou. 2020. Interfacegan: Interpreting the disentangled face representation learned by gans. *IEEE Transactions on Pattern Analysis and Machine Intelligence* (2020).
- Ivan Skorokhodov, Sergey Tulyakov, and Mohamed Elhoseiny. 2021. StyleGAN-V: A Continuous Video Generator with the Price, Image Quality and Perks of StyleGAN2.
- Ayush Tewari, Mohamed Elgharib, Gaurav Bharaj, Florian Bernard, Hans-Peter Seidel, Patrick Pérez, Michael Zollhofer, and Christian Theobalt. 2020a. Stylerig: Rigging stylegan for 3d control over portrait images. In *Proceedings of the IEEE/CVF Conference on Computer Vision and Pattern Recognition*. 6142–6151.
- Ayush Tewari, Mohamed Elgharib, Mallikarjun BR, Florian Bernard, Hans-Peter Seidel, Patrick Pérez, Michael Zollhofer, and Christian Theobalt. 2020b. PIE: Portrait Image Embedding for Semantic Control. *ACM Transactions on Graphics (Proceedings SIGGRAPH Asia)* 39, 6. <https://doi.org/10.1145/3414685.3417803>
- Yu Tian, Jian Ren, Menglei Chai, Kyle Olszewski, Xi Peng, Dimitris N. Metaxas, and Sergey Tulyakov. 2021. A Good Image Generator Is What You Need for High-Resolution Video Synthesis. In *International Conference on Learning Representations*. <https://openreview.net/forum?id=6puCSjH3hWA>
- Omer Tov, Yuval Alaluf, Yotam Nitzan, Or Patashnik, and Daniel Cohen-Or. 2021. Designing an Encoder for StyleGAN Image Manipulation. *arXiv preprint arXiv:2102.02766* (2021).
- Sergey Tulyakov, Ming-Yu Liu, Xiaodong Yang, and Jan Kautz. 2018. MoCoGAN: Decomposing motion and content for video generation. In *IEEE Conference on Computer Vision and Pattern Recognition (CVPR)*. 1526–1535.
- Rotem Tzaban, Ron Mokady, Rinon Gal, Amit H. Bermano, and Daniel Cohen-Or. 2022. Stitch it in Time: GAN-Based Facial Editing of Real Videos. <https://doi.org/10.48550/ARXIV.2201.08361>
- Kaisiyuan Wang, Qianyi Wu, Linsen Song, Zhuoqian Yang, Wayne Wu, Chen Qian, Ran He, Yu Qiao, and Chen Change Loy. 2020. MEAD: A Large-scale Audio-visual Dataset for Emotional Talking-face Generation. In *ECCV*.
- Yaohui Wang, Francois Bremond, and Antitza Dantcheva. 2021. InMoDeGAN: Interpretable Motion Decomposition Generative Adversarial Network for Video Generation. <https://doi.org/10.48550/ARXIV.2101.03049>
- Yaohui Wang, Di Yang, Francois Bremond, and Antitza Dantcheva. 2022. Latent Image Animator: Learning to Animate Images via Latent Space Navigation. In *International Conference on Learning Representations*. https://openreview.net/forum?id=7r6kDq0mK_
- Zongze Wu, Dani Lischinski, and Eli Shechtman. 2020. StyleSpace Analysis: Disentangled Controls for StyleGAN Image Generation. *arXiv preprint arXiv:2011.12799* (2020).
- Changqian Yu, Jingbo Wang, Chao Peng, Changxin Gao, Gang Yu, and Nong Sang. 2018. BiSeNet: Bilateral Segmentation Network for Real-time Semantic Segmentation.
- Fisher Yu, Yinda Zhang, Shuran Song, Ari Seff, and Jianxiong Xiao. 2015. LSUN: Construction of a Large-scale Image Dataset using Deep Learning with Humans in the Loop. *arXiv preprint arXiv:1506.03365* (2015).
- Jiapeng Zhu, Yujun Shen, Deli Zhao, and Bolei Zhou. 2020b. In-domain gan inversion for real image editing. In *European Conference on Computer Vision*. Springer, 592–608.
- Peihao Zhu, Rameen Abdal, John Femiani, and Peter Wonka. 2022. Mind the Gap: Domain Gap Control for Single Shot Domain Adaptation for Generative Adversarial Networks. In *International Conference on Learning Representations*. <https://openreview.net/forum?id=vqGi8Kp0wM>
- Peihao Zhu, Rameen Abdal, Yipeng Qin, John Femiani, and Peter Wonka. 2020a. Improved StyleGAN Embedding: Where are the Good Latents? arXiv:2012.09036 [cs.CV]